

Indirect barrier electron-hole gas transitions in mixed type-I–type-II GaAs/AlAs multiple quantum wells

R. Guliamov, E. Lifshitz, E. Cohen, and Arza Ron

Solid State Institute, Technion–Israel Institute of Technology, Haifa 32000, Israel

L. N. Pfeiffer

Bell Laboratories, Lucent Technologies, Murray Hill, New Jersey 07974

(Received 12 July 2000; published 21 June 2001)

We studied the photoluminescence (PL) spectrum resulting of the indirect recombination of barrier electrons and the two-dimensional hole gas (2DHG) that is excited in a structure of mixed type-I–type-II GaAs/AlAs quantum wells. This structure consists of alternating narrow and wide GaAs quantum wells (QW), and is distinguished by a staggered conduction-band alignment that leads to a fast electron transfer from the narrow to the wide QW's and a very slow hole transfer. Consequently, a 2DHG and a two-dimensional electron gas (2DEG) are formed in the narrow and wide QW's, respectively. Their density is controlled by the photoexcitation intensity and is experimentally determined by fitting the band shape of the wide-well direct-recombination PL spectra (in the range of $10^{10} < n_e < 5 \times 10^{11} \text{ cm}^{-2}$). A small fraction of the electrons recombine radiatively with the 2DHG while they are in the lowest X subband of the AlAs barrier, and the resulting spectrum is investigated at $T=2 \text{ K}$ and for various excitation intensities. The indirect transitions consist of a no-phonon band and momentum conserving (zone-edge) phonon sidebands. All these bands are blueshifted with increasing photoexcitation intensity. This shift is well explained by calculating the lowest X subband energy in the electrostatic potential, generated by the separate 2DEG and 2DHG charges as a function of their density.

DOI: 10.1103/PhysRevB.64.035314

PACS number(s): 78.55.Cr

I. INTRODUCTION

The interband transitions of a two-dimensional electron gas (2DEG) are usually studied in n -type modulation-doped quantum wells^{1,2} (QW). The 2DEG density (n_e) is varied either by applying a bias voltage or by photoexcitation intensity (“optical depletion”). The main spectral signatures of the 2DEG interband transitions in GaAs/Al_xGa_{1-x}As modulation-doped QW's are the reduced bandgap, as observed in the photoluminescence (PL) (band-gap renormalization) and the Burstein-Moss shift. The latter are results of the conduction-band filling that lead to the absorption threshold being at a Fermi energy above the reduced bandgap. Many studies showed that the 2DEG recombines directly with the holes that are photoexcited in the QW, and the \mathbf{k} conservation depends on the degree of hole localization.^{3,4} The transition intensity increases at the 2DEG Fermi energy (“Fermi edge singularity”) with increasing hole localization.⁵ Another consequence of the direct 2DEG-hole recombination is that the LO-phonon sidebands (PSB) are too weak to be observed in the PL spectrum. The 2DEG-hole spectrum evolves into an excitonic spectrum in the low-density limit ($n_e < 5 \times 10^{10} \text{ cm}^{-2}$) that includes both neutral and charged exciton lines.^{6,7} Finally, spectral properties that are analogous to those of the 2DEG-hole recombination are observed in p -type GaAs/Al_xGa_{1-x}As modulation-doped QW's, where the recombination is that of a two-dimensional hole gas (2DHG) with minority electrons.^{8,9} The evolution of an excitonic recombination into a 2DEG-hole or 2DHG-electron is most commonly studied in QW's with a one-component plasma and where the interband transitions are direct.

In the present study we report on the indirect recombination of a 2DHG that is confined in a GaAs QW with minority electrons that are temporarily confined in the AlAs barriers during their fast transfer process. This new type of indirect recombination is studied in an undoped, mixed type-I–type-II quantum well GaAs/AlAs (MTQW) structure.^{10,11} Spatially separated 2DEG and 2DHG are formed in the wide and narrow GaAs QW's of the MTQW structure, respectively, when it is photoexcited with an energy above the narrow QW band gap. The 2DEG shows spectroscopic (and dynamic) properties that are similar to those observed in n -type modulation-doped QW's. On the other hand, we show in this study that the 2DHG that forms in the narrow GaAs QW's recombines radiatively with electrons that are confined to the AlAs barrier (X conduction band) and have a very low density. The resulting 2DHG PL spectrum consists of indirect transitions (in both real and momentum spaces) that are very weak compared to the direct transitions of the 2DEG in the wide wells. Some of these PL bands are PSB's that involve momentum conserving phonons, similar to those observed in the indirect exciton spectrum of type-II GaAs/AlAs QW structures.^{12,13} However, this is the only similarity between the latter case in which the electrons reside in the AlAs barriers during the indirect exciton radiative lifetime, and that of the indirect X electron-2DHG transitions observed in the MTQW. We thus utilize these transitions in order to study the dependence of the X_z and X_{xy} barrier electronic states on the 2DEG and 2DHG density, as it is varied by the photoexcitation intensity. We find that the observed blueshift of these transitions and their relative intensities are well explained by the conduction band bending that

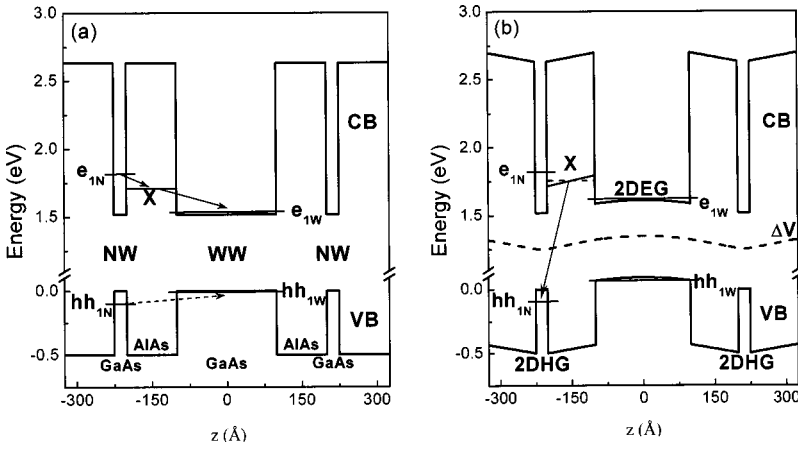


FIG. 1. (a) A schematic description of the (MTQW) structure. The lowest electron and hole subbands in the wide and narrow wells (at the Γ point), and the electron subband in the barrier (at the X point) are indicated. The electron-transfer and hole-tunneling channels are indicated by arrows. (b) The band bending caused by the 2DEG and 2DHG charges is calculated for a density of $5 \times 10^{11} \text{ cm}^{-2}$. The calculated electrostatic potential curve $\Delta V(z)$ is shown in the middle of the figure by a dashed line. The arrow indicates the recombination of a barrier-confined electron with the 2DHG in the narrow well.

is caused by the electrostatic potential of the 2DEG and 2DHG layer charges.

The paper is laid out as follows. The experimental procedures and results are discussed in Sec. II. The determination of the 2DEG and 2DHG density dependence on photoexcitation intensity is given in Sec. III. The model accounting for the indirect-transition energy dependence on the gas density is discussed in Sec. IV and Sec. V is a short summary.

II. MIXED TYPE-I-TYPE-II QUANTUM WELL STRUCTURE AND EXPERIMENTAL PROCEDURE

The MTQW structure consists of alternating narrow and wide GaAs QW's (denoted NW and WW, respectively) separated by AlAs barriers as shown schematically in Fig. 1(a). It is designed so that the lowest e_{1N} electron subband in the NW is higher in energy than the lowest X state in the AlAs barrier, leading to a type-II alignment. However, the lowest X state is higher than the e_{1W} electron subband in the WW, forming a type-I alignment. Galbraith, Dawson, and Foxon¹⁰ and Feldmann *et al.*¹¹ showed that the photoexcited electron-hole (e - h) pairs are spatially separated by the AlAs barrier. The carriers are separated since the electrons transfer rapidly from the NW to the WW through the barrier, while the holes tunnel very slowly. The initial e_{1N} - X electron transfer stage was measured to be on a subpicosecond time scale, while the subsequent X - e_{1W} electron transfer time was about 30 ps. The hole tunneling (from the hh_{1N} subband to the hh_{1W} subband) at $T=2$ K occurs in the millisecond range. Consequently, this charge separation creates a 2DEG in the WW and a 2DHG in the NW and their density can be controlled by the excitation intensity in the range $0 \leq n_e \leq 5 \times 10^{11} \text{ cm}^{-2}$. We can expect that a small fraction of the electron population remains in the barrier long enough to recombine with the 2DHG.

The MTQW structure studied here was grown by molecular-beam epitaxy on an undoped, [001]-oriented GaAs substrate. It consists of five periods of alternating wide GaAs wells ($L_{WW}=198 \text{ \AA}$) and narrow wells ($L_{NW}=26 \text{ \AA}$), separated by AlAs barriers ($L_B=102 \text{ \AA}$). The MTQW PL spectra were recorded under photoexcitation above the NW band gap [$E_L > E(e_{1N}) - E(hh_{1N})$] by an Ar⁺ laser ($E_L=2.41 \text{ eV}$), with an excitation intensity at the

sample surface of $50 \mu\text{W}/\text{cm}^2 \leq I_L \leq 50 \text{ W}/\text{cm}^2$. The sample was placed in a liquid-He Dewar and the spectra were measured at $T=2$ K. The emitted light was dispersed with a 1-m monochromator, detected with a cooled photomultiplier tube, and the signal was monitored by a lock-in amplifier.

The PL spectrum of the MTQW structure has bands in three ranges, centered around 1.52 eV (Fig. 2), 1.77 eV (Fig. 3), and 1.92 eV. These transitions correspond to direct-WW, indirect-barrier-NW, and direct-NW radiative recombination processes, respectively. Due to the rapid e_{1N} - X - e_{1W} electron transfer, the direct transitions in the NW are about 10^4 times weaker than those of the direct WW transitions. The intensity of the barrier-NW transitions is about 10^2 times weaker than that of the direct WW transitions.

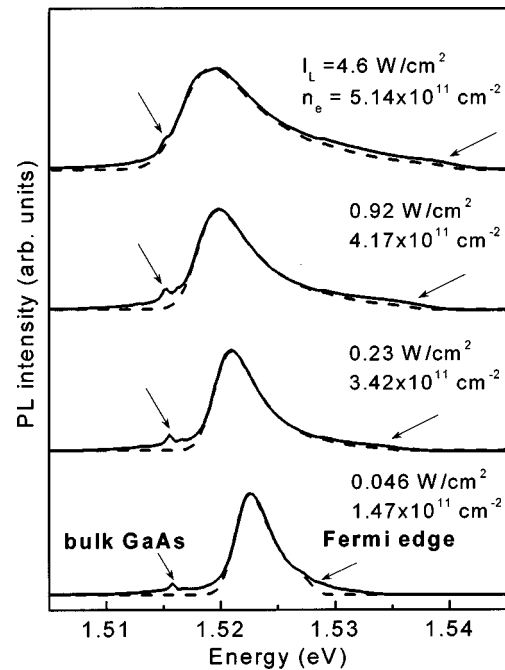


FIG. 2. PL spectra of the 2DEG in the wide QW's, observed under various excitation intensities (solid lines). The line shapes are calculated as described in the text (dashed lines). The n_e values are extracted from the line-shape fitting. The arrows indicate the Fermi-edge singularity (on the high-energy side) and the bulk GaAs PL band.

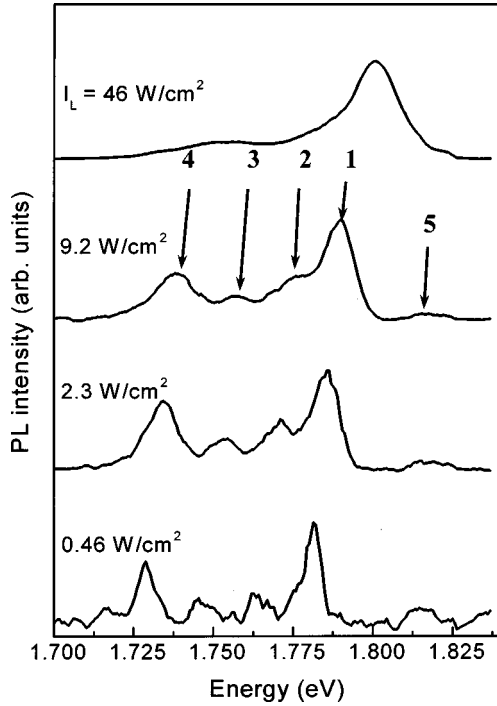


FIG. 3. PL spectra of the 2DHG in the narrow QW's that recombines with the X electrons in the barrier. The bands marked 1 and 5 are the zero-phonon indirect transitions and the other three are phonon sidebands.

Figure 2 shows the WW spectra recorded under excitation with laser intensities ranging between 0.046 and 4.6 W/cm². They all exhibit an asymmetric band, which is redshifted and broadened with increasing of I_L . They also show a weak steplike edge on the high-energy side (indicated by arrows). This weak PL enhancement is observed at the Fermi-edge singularity and it indicates that the minority holes in the WW are very weakly localized.^{3,4} The weak band at 1.515 eV is the GaAs buffer layer PL.

Figure 3 shows the barrier-NW PL spectra recorded under excitation intensities between 0.46 and 46 W/cm². They consist of five bands, which are blueshifted and change their relative intensities with increasing I_L . The band shapes were fitted to Gaussians and the extracted peak energies and integrated intensities' dependence on I_L are shown in Figs. 4(a) and 4(b). It is seen that bands 1–4 have a similar blueshift (a maximum of ~ 20 meV), while band 5 is only slightly blueshifted (~ 3 meV) followed by a redshift. Also, the intensity of bands 2–5 is reduced substantially with respect to that of band 1 at the highest I_L .

III. 2DEG- hh_{1W} PL

The WW PL spectrum, observed under laser excitation intensity $I_L < 0.01$ W/cm², exhibits exciton and trion bands.¹⁴ With increasing I_L it evolves into a single PL band that gradually becomes asymmetric and is redshifted (Fig. 2). As it is due to the 2DEG- hh_{1W} radiative recombination, its spectral shape is fitted by the following expression:^{15,16}

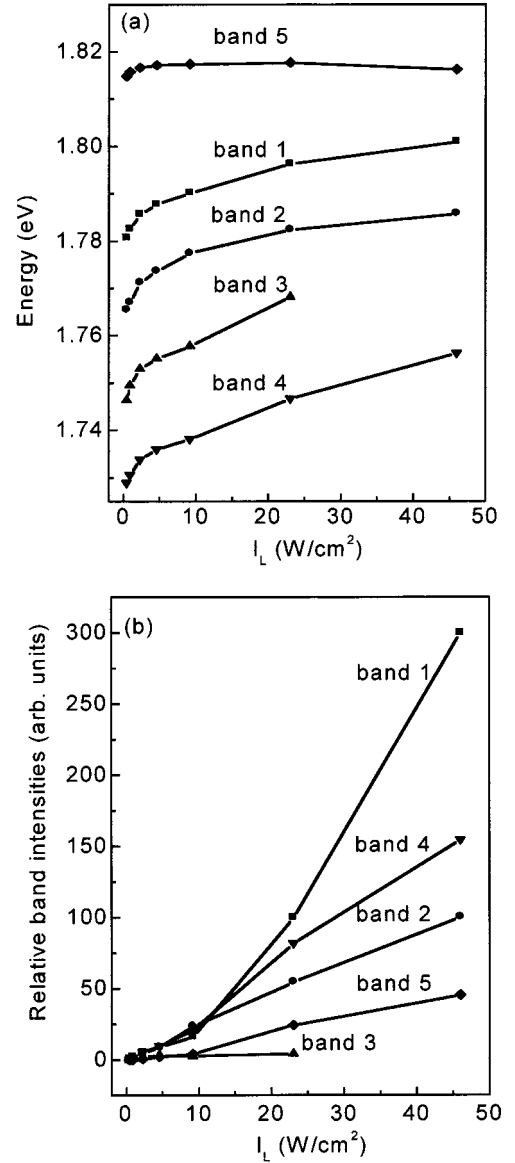


FIG. 4. Photoexcitation intensity dependence of the 2DHG PL bands. (a) Peak energy. (b) Relative integrated intensity.

$$I_{\text{PL}}(E) = A \Phi \left(\frac{E_g - E}{2\sigma} \right) \frac{1}{\exp \left[\frac{m_e}{m_e + m_k} \frac{E - E_g}{kT_k} \right]} \times \frac{1}{\exp \left[\frac{m_h}{m_e + m_k} \frac{(E - E_g) - E_F}{kT_e} \right] + 1}. \quad (1)$$

Here, $\Phi(E') = 1/2[\text{erf}(E'/\sqrt{2}) + 1]$, E_g is the renormalized band-gap energy, σ is the inhomogeneous broadening energy that is due to interface roughness, and A is a constant. The second and the third multipliers in Eq. (1) represent the hole Boltzmann distribution and the electron Fermi distribution, where E_F is the electron Fermi energy. m_e , T_e , m_h , and T_h are the effective mass and effective temperature of the elec-

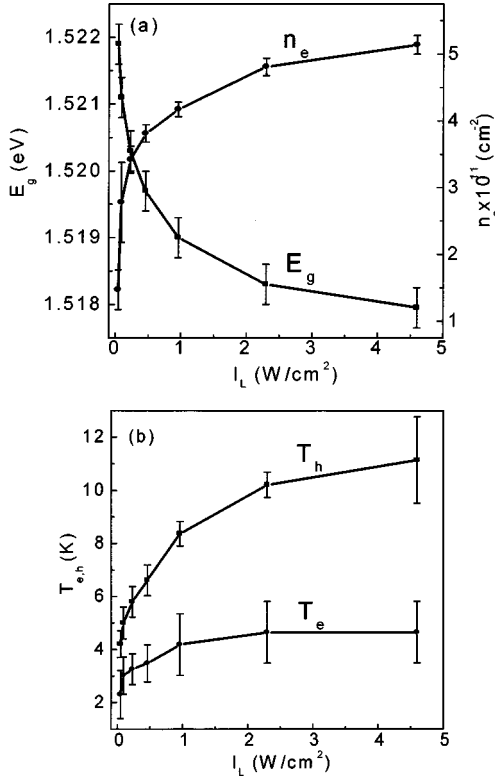


FIG. 5. Photoexcitation intensity dependence of various wide QW recombination parameters: (a) Band gap and 2DEG density. (b) Effective electron and hole temperatures.

tron and hole in the WW, respectively. The fitted PL band shapes are shown by the dashed lines in Fig. 2. The extracted dependence of the fitting parameters: n_e [using E_F (meV) = $3.6 \times 10^{-11} n_e$ (cm^{-2}) for GaAs], E_g , T_e , and T_h on I_L are plotted in Figs. 5(a) and 5(b). An increase in I_L causes a nonlinear increase in n_e and a simultaneous decrease in the value of E_g , accompanied by an increase of the electron and hole effective temperatures.

IV. 2DHG-BARRIER ELECTRON INDIRECT TRANSITIONS

As shown in Figs. 3 and 4(a), the PL spectra in the barrier-NW spectral range consist of a group of four bands that are equally blueshifted with increasing photoexcitation intensity and a fifth (highest) band that shows a different shift. We compared the spectra shown in Fig. 3 with that obtained from a type-II QW structure having a GaAs well and AlAs barrier widths of $L_W=26 \text{ \AA}$ and $L_B=102 \text{ \AA}$, respectively. The spectra are similar in their band structure but that of the type-II structure has an excitonic nature and is independent of the excitation intensity. Following the analysis of the PL bands in type-II QW's,^{12,13} band 1 is identified as the $hh_{1N}-X_{xy}$ no-phonon (ZP) indirect recombination band. The energy of bands 2, 3, and 4 appears at 13, 32, and 49 meV below that of the ZP band, respectively. These values are in close agreement with the TA, LA, and LO energies for momentum-conserving phonons in AlAs (i.e., phonons at the X point of the Brillouin zone). Thus, bands 2–4 are iden-

tified as the phonon sidebands of the $RR_{1N}-X_{xy}$ transition. The energy of band 5 is about 20 meV higher than that of band 1 and it is virtually independent of I_L . It was identified as the $hh_{1N}-X_z$ indirect recombination band of a type-II QW,^{12,13} since the X_z state lies above the X_{xy} state in AlAs barriers having a width $L_B > 60 \text{ \AA}$.¹⁷

The PL bands of a type-II QW are due to the recombination of indirect excitons formed of X electrons and hh_1 holes. Under cw photoexcitation, only excitons are formed in this QW and therefore, the PL band energies in type II do not depend on I_L . In contrast, in MTQW the observed indirect recombination of barrier electrons with the 2DHG in the NW is blueshifted with increasing excitation intensity. Since separately confined 2DEG and 2DHG are photoexcited in the MTQW structure, we attribute the PL band's blueshift to band bending that is caused by the interwell electrostatic potential. This potential is due to the charges of the separate 2DEG and 2DHG. We will now calculate the energy shift of the emitting states by solving the Poisson equation for the electrostatic potential under the following assumptions: (a) The 2DEG and 2DHG charges are equal and only $\sim 1\%$ of the electron density is trapped in the barrier and recombines with the 2DHG. This assumption is based on the very fast electron transfer through the AlAs barrier,¹⁰ and on our observation that the $hh_{1N}-X_{xy}$ transitions are about 100 times weaker than those of the WW. (b) The charge distributions within both the NW and the WW are assumed to be uniform and the barriers are uncharged. The reasons are that the hh_{1N} holes are confined to a very narrow QW and their energy distribution is mostly affected by interface roughness. The 2DEG in the WW is not involved in the indirect transitions and thus its charge distribution is immaterial. The net result is a triangularly shaped potential. (c) The n_e value for a given excitation intensity is extracted from the WW lineshape fitting.

For the calculation of the electrostatic potential we use an elementary, one-dimensional well-barrier sequence along the growth axis (z) that contains one NW, its two barriers, and two WW's (Fig. 1). In order to maintain charge neutrality we start this sequence from the middle of a WW and end it in the middle of an adjacent WW. Obviously, this sequence is repeated along the z axis in order to describe the potential of the entire MTQW structure. An example of the band bending due to the variation of an electrostatic potential, $\Delta V(z)$, along one sequence calculated for $n_e=5.1 \times 10^{11} \text{ cm}^{-2}$ is shown in Fig. 1(b).

The shifts of the X_{xy} and X_z electronic states are calculated using the triangular potential of the barrier, according to the following equation:¹⁸

$$E_n(X_{xy}, X_z) = \left[\frac{\hbar^2}{2m^*(X_{xy}, X_z)} \right]^{1/3F} \left[\frac{3\pi eF}{2} \left(n + \frac{3}{4} \right) \right]^{2/3} \quad (2)$$

Here $m^*(X_{xy})=0.19m_0$, $m^*(X_z)=1.10m_0$ (Ref. 17) and F is the electric field strength in the barrier. The calculated shifts as a function of I_L with respect to the energy at $F=0$ (namely, for $I_L=0$) are shown by solid lines in Fig. 6. The experimental shifts of bands 1–5, given with respect to their energy at $I_L \rightarrow 0$, are plotted in shaped symbols. Evi-

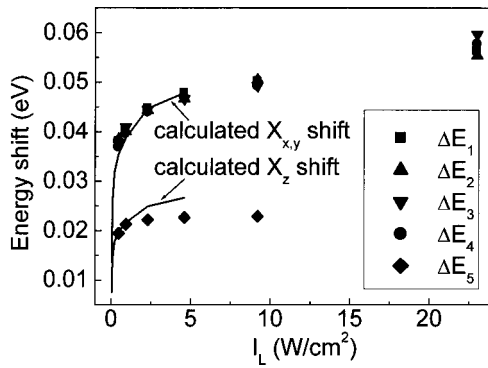


FIG. 6. Measured X_{xy} - and X_z -level shifts (symbols) as a function of photoexcitation intensity. The solid lines are calculated using a simple electrostatic model for the level shifts.

dently, there is a good agreement between the electrostatic model and the observed experimental shifts for bands 1–4. The blueshift of band 5 in MTQW is smaller than that of bands 1–4 as expected, since $m^*(X_{xy}) < m^*(X_z)$. This further supports the PL-band assignment. As Fig. 3 shows, there is an enhancement of the hh_{1N} - X_{xy} ZP transition with respect to its PSB's as I_L increases. This may be due to an admixing of the X_{xy} state with the X_z state that increases with increasing electric-field strength. The X_z state overlaps more with the hh_{1N} state than does the X_{xy} state.^{12,13}

Finally we note that the bandwidth of bands 1–4 increases considerably with increasing I_L . The inhomogeneous broad-

ening of these bands observed for $I_L \rightarrow 0$ is due to interface fluctuations (that is larger than the hole Fermi energy).

V. SUMMARY

We studied the photoluminescence spectrum that results in the recombination of a 2DHG confined to a narrow GaAs quantum well, with electrons that are temporarily confined to the AlAs barrier (X band). The 2DHG and a spatially separate 2DEG were photoexcited in a mixed type-I–type-II QW structure. Their density was varied by the excitation intensity and the charged layers induced an electrostatic potential that caused band bending. This in turn shifted the barrier subbands to higher energy and it caused a blueshift of the barrier electron-2DHG indirect transitions with increasing excitation intensity. The spectral dependence of this type of indirect transitions on the excitation intensity is very different from that observed in direct transitions of a 2DEG with minority holes that are confined to the same QW. The transition-energy shift with increasing 2DEG (and 2DHG) was calculated using a simple electrostatic model for the band bending. The photoexcited mixed type-I–type-II QW GaAs/AlAs structure is therefore suitable for the study of the dynamics of a 2DHG in very narrow QW's.

ACKNOWLEDGMENTS

The work was done at the Barbara and Norman Seiden Center for Advanced Opto-Electronics Research and was supported by the Fund for the Promotion of Research at the Technion.

- ¹S. Schmitt-Rink, D. S. Chemla, and D. A. B. Miller, *Adv. Phys.* **38**, 89 (1989).
- ²I. V. Kukushkin and V. B. Timofeev, *Adv. Phys.* **45**, 147 (1996).
- ³M. S. Skolnick, J. M. Rorison, K. J. Nash, D. J. Mowbray, P. R. Tapster, S. J. Bass, and A. D. Pitt, *Phys. Rev. Lett.* **58**, 2130 (1987).
- ⁴R. Cingolani and K. Ploog, *Adv. Phys.* **40**, 523 (1991).
- ⁵P. Hawrylak, *Phys. Rev. B* **44**, 3821 (1991).
- ⁶G. Finkelstein, H. Shtrikman, and I. Bar-Joseph, *Phys. Rev. Lett.* **74**, 976 (1995).
- ⁷A. J. Shields, M. Pepper, D. A. Ritchie, and M. Y. Simmons, *Adv. Phys.* **44**, 47 (1995).
- ⁸D. Huang, J. Chyi, and H. Morkoc, *Phys. Rev. B* **42**, 5147 (1990).
- ⁹J. Wagner, A. Ruiz, and K. Ploog, *Phys. Rev. B* **43**, 12 134 (1991).
- ¹⁰I. Galbraith, P. Dawson, and C. T. Foxon, *Phys. Rev. B* **45**, 13 499 (1992).
- ¹¹J. Feldmann, M. Preis, E. O. Göbel, P. Dawson, C. T. Foxon, and I. Galbraith, *Solid State Commun.* **83**, 245 (1992).
- ¹²P. Dawson, C. T. Foxon, and H. W. van Kesteren, *Semicond. Sci. Technol.* **5**, 54 (1990).
- ¹³M. Maaref, F. F. Charfi, D. Scalbert, C. Benoit à la Guillaume, and R. Planel, *Phys. Status Solidi A* **170**, 637 (1992).
- ¹⁴A. Manassen, E. Cohen, Arza Ron, E. Linder, and L. N. Pfeiffer, *Phys. Rev. B* **54**, 10 609 (1996).
- ¹⁵S. Munnix, D. Bimberg, D. E. Mars, J. N. Miller, E. C. Larkins, and J. S. Harris, *Superlattices Microstruct.* **6**, 369 (1989).
- ¹⁶J. Christen and D. Bimberg, *Phys. Rev. B* **42**, 7213 (1990).
- ¹⁷H. W. van Kesteren, E. C. Cosman, P. Dawson, K. J. Moore, and C. T. Foxon, *Phys. Rev. B* **39**, 13 426 (1989).
- ¹⁸C. Weisbuch and B. Vinter, *Quantum Semiconductor Structures—Fundamentals and Applications* (Academic, San Diego, 1991), p. 20.